High Resolution Elevation Data Derived from Stereoscopic CORONA Imagery with Minimal Ground Control: An Approach Using Ikonos and SRTM Data

Nikolaos Galiatsatos, Daniel N.M. Donoghue, and Graham Philip

Abstract

The first space mission to provide stereoscopic imagery of the Earth's surface was from the American CORONA spy satellite program from which it is possible to generate Digital Elevation Models (DEMs). CORONA imagery and derived DEMs are of most value in areas where conventional topographic maps are of poor quality, but the problem has been that until recently, it was difficult to assess their accuracy. This paper presents a methodology to create a high quality DEM from CORONA imagery using horizontal ground control derived from Ikonos space imagery and vertical ground control from map-based contour lines. Such DEMs can be produced without the need for field-based ground control measurements which is an advantage in many parts of world where ground surveying is difficult. Knowledge of CORONA image distortions, satellite geometry, ground resolution, and film scanning are important factors that can affect the DEM extraction process. A study area in Syria is used to demonstrate the method, and Shuttle Radar Topography Mission (SRTM) data is used to perform quantitative and qualitative accuracy assessment of the automatically extracted DEM. The SRTM data has enormous importance for validating the quality of CORONA DEMs, and so, unlocking the potential of a largely untapped part of the archive. We conclude that CORONA data can produce unbiased, high-resolution DEM data which may be valuable for researchers working in countries where topographic data is difficult to obtain.

Introduction

The first space satellite to provide stereoscopic images of the Earth was CORONA mission 9031 on 27 February 1962. The panoramic camera design (KH-4) of that mission provided along-track stereopairs of panchromatic images with a ground resolution of approximately 8 m. During the 1960s and early 1970s the CORONA satellite program was the United States' main intelligence gathering satellite system, and image quality and endurance were continually improved. The stereoscopic capability was enhanced with the sensor designs KH-4A and KH-4B which provided improved ground resolution and internal motion compensation.

Today, CORONA imagery is enjoying a renaissance of interest, particularly from archaeologists and environmental scientists, because the images cover a large part of the Earth's surface at high spatial resolution. The images are inexpensive, easy to acquire, and cover many parts of the world where it is difficult to obtain any other source of high-resolution imagery. CORONA images are immensely useful for identifying changes in our landscape over a period of up to four decades. In fact, the availability of new digital high-resolution spaceborne imagery has stimulated scholarly interest in CORONA data, which offers a key source of high resolution data on past landscapes and which can be used in comparative studies. However, the majority of recently published papers that have made use of CORONA data have not taken advantage of its stereoscopic capability nor have they highlighted the importance of the technical developments that accompanied each new mission, e.g., Fowler (2004), Ratcliffe and Henebry (2004), Philip *et al.* (2002a), and Ur (2003). There are, however, a number of researchers who have explored the stereoscopic potential of CORONA imagery. Pournelle and Hunt (personal communication, 2002) explored use of panoramic camera models in commercially available software packages but were unable to find one suitable for CORONA KH-4B data for a study of Iraq. Shin (2003) developed a rigorous panoramic model for CORONA KH-4A imagery to detect glacier change in Greenland, but this approach requires ground control and specialist software. Altmaier and Kany (2002) used the non-metric camera model in the OrthoBASE® module of ERDAS Imagine® to extract a DEM from CORONA KH-4B data in a mountainous landscape in southern Morocco. They used DGPS-measured ground control points (GCPs) for horizontal and vertical control. Schmidt *et al.* (2001a) created a DEM from CORONA imagery with the use of VirtuoZo software in the same area of Southern Morocco; the accuracy reported was close to that obtained by Altmaier and Kany (2002).

Nikolaos Galiatsatos and Daniel N.M. Donoghue are with the University of Durham, Department of Geography, South Road, Durham DH1 3LE, UK (nikolaos.galiatsatos@durham.ac.uk).

Graham Philip is with the University of Durham, Department of Archaeology, South Road, Durham, DH1 3LE, UK.

Photogrammetric Engineering & Remote Sensing
Vol. 74, No. 9, September 2008, pp. 1093–1106.

0099-1112/08/7409–1093/$3.00/0

These researchers cooperated on other papers (Goossens *et al.*, 2001; Schmidt *et al.*, 2001b) and used GCPs derived from the same DGPS measurements (Goossens, personal communication, 2004). The above Morocco studies reported errors simply in terms of root mean square error (RMSE), without further analysis or comparison with independently measured heights.

Schneider *et al.* (2001) used a software package developed by the University of Hanover (BLUH – Bundle Block Adjustment University of Hanover) to extract a DEM from CORONA KH-4A data. The approach combines panoramic image rectification with automatic tie point matching of stereo pairs to help produce a DEM. The accuracy of the DEM obtained by this method is reported as $RMSE_X$ = 27.6 m, $RMSE_Y$ = 19.7 m, and $RMSE_Z$ = 14.2 m (16 control points).

There are many reasons why CORONA data have not been used to derive height information on a routine basis. First, the KH-4 camera and its successors was a HYAC (for "high acuity") panoramic system which produced non-planar image geometry; it was designed to allow a large footprint to be imaged at high spatial resolution for intelligence purposes. The geometric rectification can be carried out using satellite ephemeris data (Selander, 1997) or using ground control (Schmidt *et al.*, 2001a). To use CORONA data quantitatively, it is important to have good ground data or an independent source of accurate horizontal and vertical control. Unfortunately, it is often the case that in those areas where CORONA is most useful such data either does not exist or is of restricted availability. In this paper, we use an area in the Middle East to demonstrate that many of the barriers inhibiting the exploitation of CORONA height data can be removed by the synergistic use of CORONA, Ikonos, and Shuttle Radar Topography Mission (SRTM) data.

This paper focuses on three important aspects of stereoscopic CORONA space photography. (a) Each CORONA mission was subtly different, and this can impact of stereoscopic potential and the steps required for image pre-processing; (b) The extraction of DEM data from CORONA imagery without field-based ground control measurements; and (c) the evaluation of CORONA-derived DEMs using the SRTM three arcsec interferometric radar data.

Study Area

The present study area is located in the Orontes Valley region of Syria, west of the city of Homs. CORONA data for this region was acquired as part of a program of archaeological prospection within an area covering approximately 700 km^2, wherein the nature, scale, and distribution of the archaeological resource were poorly documented. This research formed part of a Syrian-British co-operative project Settlement and Landscape Development in the Homs Region, Syria which was organized jointly by the Directorate General of Antiquities and Museums of Syria (DGAM) and Durham University (Philip *et al.*, 2002b and 2005). Height data can greatly assist the process of locating and interpreting potential sites from imagery either directly as in the case of tells[1] or indirectly by providing a landscape context. One of the aims of the project was to compare the capability of CORONA imagery with existing topographic mapping (at 1:25 000 scale) because the work of prospection required the detection of subtle features such as low tells, small standing structures, and river terraces. The study also describes a methodology that could easily be applied to many parts of the world. The project embraces two topographically distinct units, the Southern and Northern Study Areas. The Southern Study Area is composed of marls and slopes gently but steadily from the south to east where it attains heights of approximately 700 m, to Lake Qatina which is part of the Orontes Valley at an altitude of approximately 500 m. Several shallow, meandering dry valleys run across the area from south to east to north to west. The Northern Study Area consists of a continuation of the marl in the east, which is separated by the shallow trough of the Orontes Valley from a boulder-covered basaltic landscape to the west. The latter consists of a series of low ridges separated by shallow basins and has an altitudinal range of approximately 300 to 500 m. There has been very little urban development in the study area apart from around the town on Homs (which is not included in the test areas). The landscape is predominantly agricultural with isolated orchards and lines of trees forming windbreaks. Apart from a few isolated low level buildings, there has been little change in the height of surface features between 1970 (CORONA acquisition) and 2000 (SRTM acquisition). This landscape contrasts with the relatively steep terrain of Morocco (Altmaier and Kany, 2002) and Greenland (Shin, 2003). For more details on the study area, see Philip *et al.* (2002b).

[1]One of the main categories of an archaeological site in the area is the *tell*. Such sites are formed by repeated occupation at a particular location which results in the gradual build-up of mudbrick debris, and so, stand out against the relatively flat landscape.

Data

CORONA Imagery

Although several books about CORONA have been published, e.g., Ruffner (1995), Peebles (1997), McDonald (1995 and 1997), and Day *et al.* (1998), all of them focus on the history of the CORONA project rather than detailing the technical characteristics of the cameras and their potential for deriving height data from stereoscopy. The stereo potential of CORONA can be seen from the high ground resolution and the base/height (B/H) ratio. The ground resolution reaches 1.8 m in KH-4B, and this improves recognition of GCPs. With simple triangulation, one can easily show that the B/H ratio of CORONA is 0.54, very near the suggested lower limit of 0.6 needed to meet the requirements of topographical mapping (Slama *et al.*, 1980). Galiatsatos (2004) has shown that it is wrong to assume that each CORONA mission was equipped with a similar camera design and setup. The major changes in ITEK™ camera design are well documented (e.g., Madden, 1996) but what is less well appreciated is that mission scientists continually experimented with the cameras, films, filters, slits, lenses, and many other parts of the satellite systems. The precise details of each mission are difficult to obtain, but in our case information was taken from declassified CORONA documents such as National Reconnaissance Office (NRO) (NRO, 1970a and 1970b) which list the specific characteristics of the imagery used in this paper (Table 1). The study area was covered by three stereopairs, and so six areas of interest were extracted from the full image strip (757 mm by 70 mm) each approximately 100 mm by 70 mm in size. The areas of interest in this particular case were centred at an angle of approximately 18° off-nadir; note that the center line of a CORONA image strip (i.e., the long axis of each strip of KH-4B film) is always 15° off-nadir because of the tilt of the camera, see Figure 1.

Table 1 shows that the two cameras used in Mission 1110 had different generation lenses; the forward camera had

TABLE 1. SATELLITE SYSTEM CONFIGURATION FOR THE IMAGERY USED IN THIS PROJECT

Mission	Cameras	Frame No.	Date	Petzval	Film	Filters[$]
1110	Fwd	07,08,09	28/05/1970	Type II	3404/14*	21/23A
1110	Aft	13,14,15	28/05/1970	Type III	3404/14*	23A/25

[$]Prime/Alternate. The most likely filter for the images in the project is the prime. There is uncertainty.
*3414 film was spliced-in. There is uncertainty if the film of the project was 3404 or 3414. Most probably it was 3404. (The alternate filter was glass filter 0.007 inch for increase of 0.001 inch in focus.)

a second generation and the aft camera a third generation petzval lens. This has an impact on the film resolution. According to NRO (1970a), the performance nadir prediction of the second generation lens is 130 line pairs per millimeter (lp/mm) and the third generation lens is 155 lp/mm (for a 2.44 msec exposure time, 3404 film type, 2:1 contrast, field angle 0°, and 152 km altitude). This film resolution shows that the film granules resolve at 3.8 and 3.2 μm, respectively. For Mission 1110, the overall image quality is less than that provided by previous KH-4B missions (Peebles, 1997).

There is some uncertainty about the heritage of the CORONA film products; we assume that a direct copy of the original film was supplied by Kodak to the United States Geological Survey (USGS) to archive and to copy for those who request imagery. The term "original" refers to the closest to the original generation of film that the intelligence community was able to locate for inclusion in the USGS collection (McDonald, 1997). Hence, it is likely that the film may have been copied more than twice before being prepared for digital photogrammetric scanning (Ruffner, 1995). The frames of the index, horizon, and stellar cameras are not declassified.

Figure 1 shows the bow-tie shape of the CORONA panoramic camera footprint and the basic CORONA system geometry from KH-4 (27 February 1962) onwards. The inserts show in plan-view the nature of the geometric

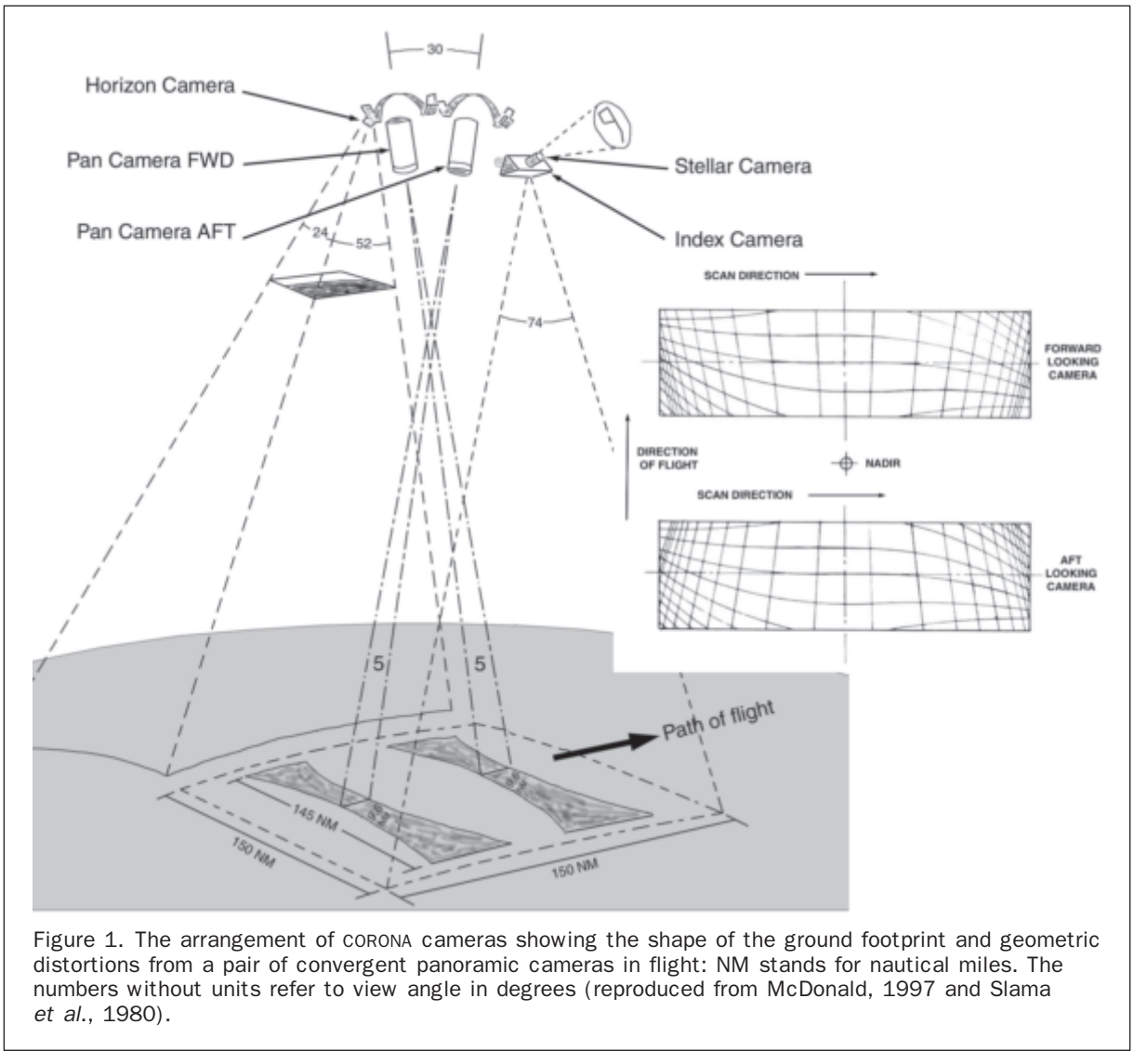

Figure 1. The arrangement of CORONA cameras showing the shape of the ground footprint and geometric distortions from a pair of convergent panoramic cameras in flight: NM stands for nautical miles. The numbers without units refer to view angle in degrees (reproduced from McDonald, 1997 and Slama *et al.*, 1980).

distortions contained in the fore and aft stereo camera. Notice how the image scale changes from the nadir towards the edges. These distortions can be corrected by a rigorous mathematical transformation or empirically using ground control. Sohn *et al.* (2004), Schenk *et al.* (2003), and Shin (2003) used a rigorous approach for processing CORONA photography. Panoramic photography was an innovative and fashionable method developed for aerial survey in the 1950s to 1970s, but it is little used today. The best source of information about these cameras is from publications such as Slama *et al.* (1980) which describe the concepts and the correction of the image data. Note that some of the authors in Slama *et al.* (1980) were involved in the CORONA program. Other publications relevant to the CORONA panoramic cameras are Case (1967) and Devereaux (1973).

From the above publications, the most important point to emerge is that if there is sufficient ground control then the ephemeris data are not required (Ondrejka, personal communication, 2000; Slama *et al.*, 1980).

Scanning

Leachtenauer *et al.* (1997) describe an experiment that tested a sample of CORONA data with both commercial and prototype scanners. They found that the images could be digitized with no loss of information content, but to do so, required using a very small digitizing spot of 4 μm, which took substantial time and produced large digital files. Thom (2002) shows that the smaller the step of scan, the better will be the precision and the spatial resolution, but there may also be loss of radiometric precision. In practical applications, the impact of radiometric quality on the geometric precision is not easy to evaluate. Generally, weakly contrasted details can be separated when attention has been given to the radiometric quality. Figure 2 shows an extract from a CORONA image scanned with two different contrast settings. It demonstrates that for high contrast scenes the radiometry can affect manual interpretability and probably the feature matching required for the automatic DEM extraction.

This research project used a Vexcel VX4000 photogrammetric scanner to digitize all images at the optimal 7.5 μm (about 3,400 dpi) optical resolution. This is the highest optical resolution that this scanner can achieve. This scanner was owned and operated by a private company and was radiometrically and geometrically calibrated before the scans took place. We noted that the fore and aft pointing cameras produced images with different contrast because of the sun-camera-surface geometry, and so care was taken with the contrast settings when scanning image stereopairs.

In all CORONA DEMs, we noticed horizontal stripes or bands running perpendicular to the flight direction of the satellite (see the top right hand image in Figure 3). The source of the banding effect was traced to the digital imagery, although it is not at all evident in normal image display. A feint regular grid pattern was identified when the imagery was enhanced with a 3×3 spatial convolution standard deviation filter (see the top left hand image in Figure 3). This filter highlights image texture and is useful for detecting defects in image quality. The lower image in Figure 3 shows that the grid pattern in the imagery is collocated with the stripes observed in the DEM. The standard deviation filter was applied to all of our scanned CORONA images to try to identify the source of the grid; the grid appeared in all images. The film negatives obtained from the USGS were then checked on a light table with a magnifying glass, and no grid could be detected. From this, we assume that the source of the grid is the digital scanning.

Kasser (2002) points out that even if a calibration is applied to the scanner, some irregularities may persist. For example, calibration errors or dust particles will affect the radiometric precision of the scanning. In particular for matrix CCD scanners, there will be periodic and annoying artifacts due to repetition of errors according to a regular paving, and of radiometric discontinuities between successive positions of the matrix.

Whatever the reason is for this striping, its effect is transferred to the height model by the ERDAS method for automatic DEM extraction. The grid influences the stripes only in one direction because height is a function of *x*-parallax, and therefore no stripes occur in *y*-axis of the grid. The problem may be due to insufficient radiometric/geometric calibration of the photogrammetric scanner.

Tappan *et al.* (2000) preferred to photointerpret CORONA straight from the film without any digitizing. This is a rigorous approach, but it inhibits the GIS potential of data integration. Bindschadler and Vornberger (1998) scanned

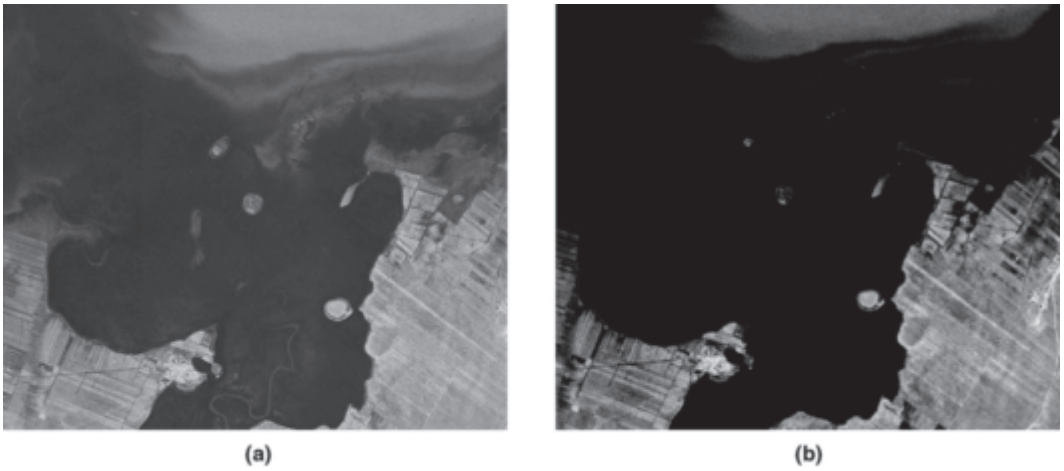

Figure 2. Effect of digitizer setup over a high contrast site (a) with regard to radiometric detail, and (b) with regard to geometric precision.

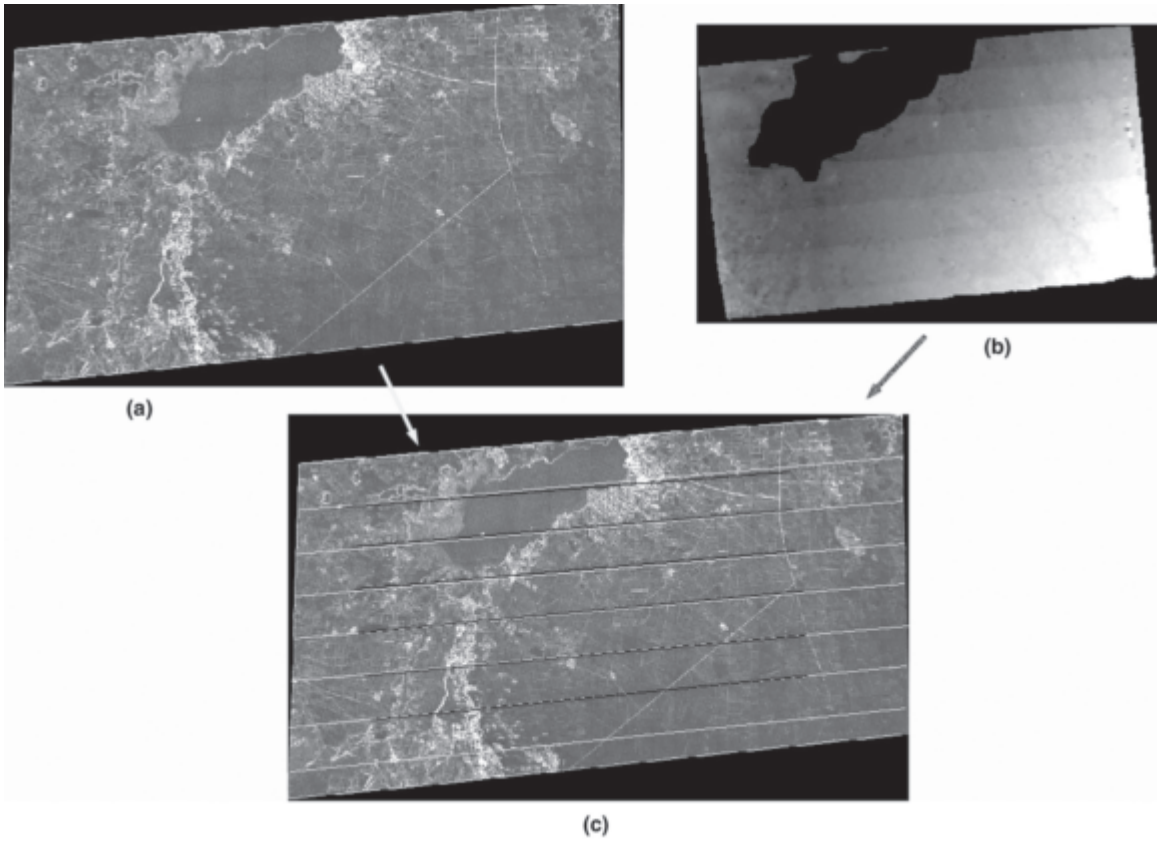

Figure 3. Image (c) shows that the "grid effect" CORONA image (a) correlates with the stripes in the CORONA DEM (b). A color version of this figure is available at the ASPRS website: **www.asprs.org**.

the film to a satisfactory scale for their application, while Palmer (2002) preferred to create large scale photographic prints and then process these on a flatbed scanner. Palmer's approach is simple but effective and demonstrates that for certain applications, complex data pre-processing may not be necessary. Note that, since 03 September 2004, USGS ceased film products provision. Hence, all CORONA data are now scanned by the USGS.

Ground Control

In many parts of the world, it is difficult to obtain ground control, either from published map sources, aerial photographs, or ground survey techniques. In this study, we required horizontal control to correct for the image distortion and to orientate the final DEM to a recognized map projection, and we required vertical control for common points on stereopairs to calculate the interior and exterior orientation parameters using a bundle block adjustment method. We also require an independent source of height information to provide an independent check on the height information derived from the photogrammetry.

According to Gerlach (2000), the positional accuracy of the Ikonos "standard geometrically corrected" level 1 product is 23.3 m RMSE, not including the effects of terrain displacement. According to the latest Ikonos product guide (Space Imaging, 2005); the positional accuracy of the "Geo" product is 15.0 m CE90, exclusive of terrain effects. From GPS measurements in the area of interest during summer 2002, it became apparent that the Ikonos accuracy could be as good as 10 m RMSE (Beck *et al.*, 2005). It should be noted that Ikonos is a satellite sensor with an imaging system free of significant non-linearities (Fraser *et al.*, 2002). The information content of Ikonos can provide an ideal base layer for the rest of the data. Davis and Wang (2003) proved that with enough data to create an Ikonos orthoimage, then the planimetric accuracy would be suitable for its use as a base layer.

In this study, we used the Ikonos Geo product imagery, acquired on 03 February 2002, in both panchromatic and multispectral modes with a spatial resolution of one and four meters, respectively. When we acquired the Ikonos Geo product imagery, the RPCs (Rational Polynomial Coefficients) were not available for this product. Hence, the imagery could not be further corrected with the use of RPCs. However, it still proved highly accurate as explained above.

In this study, and with the particular data, the error due to planetary curvature is negligible (Slama *et al.*, 1980); hence a correction for planetary curvature was not included.

Validation Data from SRTM Three Arcsec

On 01 April 2004, NASA (National Aeronautics Space Administration) published the SRTM (Shuttle Radar Topography Mission) three arc-second data of Homs area on the World-Wide-Web. The data are free to download in .hgt format from **ftp://e0mss21u.ecs.nasa.gov/srtm/**. Flown aboard the NASA Space Shuttle Endeavour on 11–22 February 2000, the SRTM successfully collected data over 80 percent of the Earth's land surface, for most of the area between 60°N. and 56°S. latitude.

The SRTM three arcsec DEM is a particularly valuable source of height data for parts of the world where topographic maps are not readily available. The most up-to-date

information suggests that its vertical accuracy is approximately 5 m, depending on the relief of the ground (Farr, 2004). However, various applications from Hungary (Kay *et al.*, 2005), Portugal (Gonçalves and Fernandes, 2005), and Turkey (Jacobsen, 2005) have all demonstrated an accuracy of less than 5 m in a variety of terrain. The SRTM one arcsec is not yet available outside the United States. A detailed description of the SRTM as well as an evaluation of the DEM product quality can be found in Rabus *et al.* (2003).

Rectification of CORONA Imagery

The cameras used on CORONA missions produced panoramic satellite stereo images that were intended to assist manual photo interpretation. Unlike modern satellite stereo image data, it is difficult to obtain the parameters needed to perform a rigorous analysis of digital data to extract height information. As in many parts of the world, it was difficult to take Differential Global Positioning System (DGPS) measurements in our study area because of military restrictions, while access to accurate coordinates and basemaps was also problematic. For these reasons an approach was followed that used a combination of Ikonos, map, and SRTM three arcsec data. Table 2 shows the geometric properties of Ikonos Panchromatic (1 m spatial resolution) Geo product images acquired over the study area on 03 February 2002. There are two issues here that are illustrated in Figure 4. First, Ikonos does not completely cover the area of the CORONA images (notice stereopair 008-014), thus restricting the horizontal control. However, the GCPs were equally distributed and the overlap was exploited in full. Second, the Ikonos comes in two parts with different geometry and scan directions, which creates a divided base-layer. When the scan direction is *forward*, then the scan and the orbital velocity vectors are pointing in the opposite directions (Grodecki *et al.*, 2003). For this reason, the metadata angles of the *forward* mode should not be used for orthorectification or other geometric corrections.

TABLE 2. GEOMETRY OF CORONA AND IKONOS IMAGERY USED IN THIS PROJECT

Ikonos	Scan Azimuth	Scan Direction	Collection Azimuth	Collection Elevation
756	179.97°	Reverse	38.3713°	67.22347°
757	359.96°	Forward	67.8092°	76.36649°
CORONA	Camera Looking	Scan Direction*	Orbit Inclination	Sensor Elevation
009fwd	Backward	Anticlockwise	83°	74.77°
015aft	Forward	Clockwise	83°	74.77°

*Looking from behind the satellite.

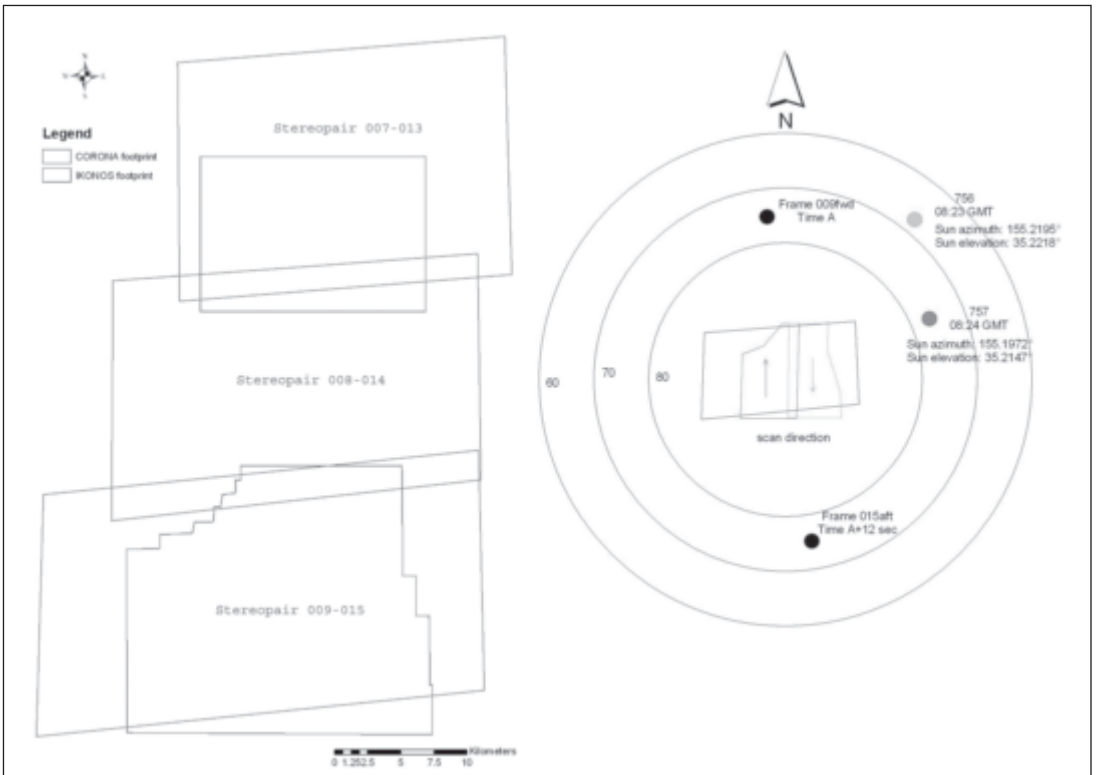

Figure 4. CORONA and Ikonos image locations and the scan directions in polar co-ordinates display for the 009-015 stereopair and the south part of Ikonos imagery. A color version of this figure is available at the ASPRS website: **www.asprs.org**.

Furthermore, there is a need to generate height information for GCPs (Ground Control Points), something that is not included in the Ikonos Geo product. For this, a series of 1:25 000 Syrian maps were registered to Ikonos, and after registration, the heights were sampled from the contour lines. This assumes that the contour lines were produced accurately. The contour interval is 5 m and there are spot heights in various places within the maps. The registration accuracy of maps to Ikonos was done with care and achieved sub-pixel accuracy. The reader would naturally assume that the spatial reference would be the maps, but not in this case. As we explained above, it was not possible to get information regarding the coordinate system of the maps. For this, we used Ikonos as a base layer in this study. Because the Ikonos Geo product lacks height information, we had to extract the heights from the maps. So as to do this, the maps had to be registered on Ikonos imagery, and not vice versa.

Nevertheless, by using the Ikonos Geo product imagery as horizontal control and the registered-to-Ikonos maps as vertical control, the CORONA geometry distortions are significantly reduced.

Initially, the panoramic camera model in the SocetSet™ software package was used to establish the geometric relationship between the stereo pairs. However, the best results using the rigorous approach of the available sensor modeling gave a uniform error of around 160 pixels to all points of one image and about 20 pixels to all points in the other image. In particular, the total RMSE was about 20 m in each direction, but the specific residuals were more than 1,000 m. The reasons for this error are unknown. It is possible the error comes from the panoramic camera parameters many of which are not known precisely because of the CORONA declassification process. The values of some of the parameters, such as orientation, angles can play an important role in the analysis. Unfortunately, the algorithms of the panoramic model used by SocetSet™ are not known, thus it was not possible to understand or explain the source of our large errors. After contacting the SocetSet™ engineers (personal communication, 2005), they said that the Panoramic sensor model in SocetSet™ was developed with airborne sensors in mind, and that while the CORONA imagery should not be too dissimilar in theory, the practice may be different (which would lead to the *strange* results you have encountered). None of the engineers we spoke to had ever used the Panoramic model with CORONA data. After discussion with Pournelle and Hunt (personal communication, 2002) who had tried all available models (even SocetSet™), it seems that the available panoramic film models, like those for frame cameras, presume boundaries on altitude and incidence angles that cannot work for orbital satellite platforms. Thus, the models presume a trapezoidal re-projection, which is not the case with CORONA.

ERDAS OrthoBase® Pro is a module included in the ERDAS Imagine® software (renamed to Leica Photogrammetry Suite in version 8.7). Like SocetSet™, it includes sensor modeling to establish the internal characteristics associated with a specific camera or sensor with its main purpose being the orthorectification of the imagery. However, ERDAS has no panoramic camera model and so the only option is to use the non-metric camera model. In the non-metric camera model, the minimum requirements are an approximate focal length (609.602 mm, from NRO, 1967) and the scanning resolution used to digitize the film. The coordinate system is defined according to the GCPs. The most difficult task was to allocate common points between the Ikonos imagery and the CORONA imagery because of the 30 year time difference and physical changes to the landscape. It was also difficult to find common points between the maps and the Ikonos imagery. The first step was registration of CORONA to Ikonos and maps to Ikonos with the use of the Geometric Correction tool of ERDAS Imagine®, thus identifying the GCPs. The height information was derived from the maps, using simultaneous display of the three data sources (maps, CORONA, and Ikonos).

Afterwards, it was straightforward to put the same points in the CORONA imagery and create a first approximation of the geometric relationship between the image and the ground. The next step was the automatic tie point creation (correlation threshold 0.65), which improved further the triangulation model.

Automatic DEM Extraction

ERDAS OrthoBase® Pro automatically creates a DEM in three steps. First, it applies a digital image matching for DEM mass point collection. With the use of Förstner interest operator (Förstner and Gülch, 1987), it identifies a series of feature points such as road intersections or centers of circular features on each image (left and right) of the pair. The cross-correlation coefficients are calculated for each matching feature point, and the points with the higher correlation (0.8 to 1.0) are chosen as a matching pair. In other words, it utilizes a feature-based matching technique, but it also uses the topological and geometrical relationships among the features. The parameters of the digital image matching can be customized according to each user's needs. Among the parameters, the search window size, the correlation window size and the correlation coefficient limit have the most influence on automatic image matching. In this study, the default parameters were kept. Whenever we used customized parameters, this is mentioned in the text.

The second step is the ground point coordinate determination. From the first step, a set of points is chosen in the left and right images. With the use of the space forward intersection technique, the ground coordinates of the points are computed to produce the mass points which are then used as a basis for the third step, the DEM construction.

Before beginning DEM extraction, some common parameters were applied to all stereopairs. A trim frame of 2.5 percent is applied to all overlaps. The trimming occurs after the mass points are extracted and before the DEM generation. Thus, the DEM is clipped to remove less accurate edges. The correlation area is reduced by a 5 percent frame, thus preventing the extraction of erroneous mass points that may be present at the edges of the images. The reduction occurs before the extraction of mass points.

The DEM image file pixel size was chosen to be 17 m to enable a minimum interest operator size[2]. The contour line spacing was chosen to be 10 m. Because of problems caused in the DEM extraction, all clouds and their shadows were excluded from the extraction, hence they appear as "islands" in the DEM. The extraction strategy was chosen to be flat areas[3] strategy with adaptive change applied.

No filtering or other interpolation techniques were applied to improve the DEM. Table 3 provides a summary of

[2]The methodology of the software for the DEM extraction requires a DEM cell size equal or higher to the maximal correlation window size, whose side has size of seven pixels. Thus, the DEM cell size could not be less than seven pixels in size. The orthorectified image pixel size was 2.3 m.

[3]In flat areas the search size is 7 × 3 pixels, which is adequate because of the absence of errors caused by high relief.

TABLE 3. STATISTICAL SUMMARY OF THE DEM AUTOMATIC EXTRACTION

	007-013	008-014	009-015
Number of tie points	14	21	0
Number of GCPS	11	11	13
Minimum, maximum error	−7.243 m, 5.715 m	−10.846 m, 10.506 m	−7.622 m, 3.816 m
Mean error, mean absolute error‡	−0.864 m, 2.766 m	−0.732 m, 3.624 m	−1.726 m, 2.905 m
$RMSE_Z$, LE90, NIMA LE90*	3.377, 5.476, ±3.189	4.461, 6.188, ±4.280	3.830, 7.014, ±4.109
General mass point quality	71.81% versus 28.19%	70.42% versus 29.58%	67.03% versus 32.97%

*$RMSE_Z$ is a global indicator of the quality of the output DEM. LE90 is a measure of vertical accuracy, and is based on mean sea level. It assumes that 90 percent of the values are within the standard deviation. NIMA LE90 is computed using the formula $\pm 1.646 * \sigma_x$

‡ Mean error is an indicator of the DEM's inclination towards positive or negative values. The mean absolute error is useful to determine the average accuracy of the extracted DEM.

the statistics associated with the DEM extraction including the mass point quality.

It should be noted that no further editing was done to the resulting CORONA DEM, for example to eliminate surface features or problematic pixels. The automatically extracted un-edited DEM is assessed in the following section.

Assessment and Discussion

Polidori (2002) points out that it is difficult to assess the accuracy and quality of a DEM in a quantitative way but suggests that the following criteria/questions are important (a) are the number of reference points good enough for the validation of the DEM extraction?; (b) What errors may be associated with the reference points?; (c) What level of accuracy is required for the application?; and (d) Are data available of sufficient quality to validate the results? In this study the number of ground reference points obtained was the best possible under the circumstances, given the local restrictions on surveying and the use of differential GPS in particular. Raw Ikonos Geo product imagery was used as a horizontal reference and the contour lines of the maps were used as a height reference. Because of the difference in time and information content between the historical CORONA and modern Ikonos imagery, it was very difficult to define common identifiable points. This is a practical limitation of the method and its impact will vary from place to place depending on the degree of landscape change.

To address Polidori's second question, the maps were registered to the Ikonos Geo product and so there will be a horizontal error included in the height data. The difference in the Ikonos scan mode (see Table 2) may incorporate extra errors. It should be noted that in the case of the 008-014 stereopair, some of the reference points were sampled from the CORONA imagery that was registered to the Ikonos scene because of the lack of adequate control for the triangulation process. Therefore, any geometric registration errors will be transferred to the DEM extraction. Perhaps this explains the magnitude of error in this stereopair compared with the other two (see Table 3) even though this pair used more reference points. It is likely that the validation data will also contain errors. In this case, the SRTM three arcsec data has been used in its published form. Missing data have been omitted from the evaluation but the data has been smoothed as part of the processing.

In summary, it is vital to be aware of the possible sources of error in the process of generating DEMs.

The third question explores the issue of the precision of the DEM and its appropriateness for the given application. In this case, archaeologists are interested in topographic features, tells, and low settlement mounds, for example, and natural landscape features, such as wadis and river terraces (Philip *et al.* 2002a). It is important to know if such features could be identified on automatically extracted DEMs because in many parts of the developing world there are no systematic surveys of archaeological remains nor ready access to aerial photography or topographic mapping at scales greater than 1:50 000. Figure 5 illustrates that the CORONA DEM contains considerably more information than the published SRTM three arcsec version, but it also illustrates that the automatically extracted DEM is not able to resolve every known archaeological tell feature, even though height differences can be observed using a stereoscope. It would be interesting to apply the methodology described by Menze *et al.* (2006) for tell detection. On the other hand, landscape features such as river channels and ridges can be distinguished easily, see Figure 5b.

The last question explores the availability of independent height information that can be used to validate the results. Most published papers use statistics such as RMSE, mean error, and absolute error to describe the quality of the DEM. The drawback with this approach is that the statistics only relate to a few measured control points. Other authors are more rigorous and use independent control points for validation. In this study, we did not have the luxury of large numbers of ground control points, and so reporting accuracy in this way (see Table 3) may be very misleading because of the small number of reference points and the hidden errors described earlier.

During September 2002, Bridgland *et al.* (2003) used differential GPS points to measure river terrace features. They established their points with the use of a base GPS of known coordinates and a "rover" GPS. As these points were not taken at *sensitive* areas (e.g., bridges, crossroads), some GPS work was permitted by the Syrian authorities. For this very reason, of course, it is impossible to identify the points precisely on the imagery. It was, however, possible to detect these points from their Easting and Northing coordinates (thus ignoring possible horizontal mismatch), and then compare their height with the height information taken from the CORONA stereopairs. The correlation was r = 0.9954 (Figure 6), and the spatial relationship for points located widely over the study area showed no obvious bias.

An alternative approach is to compare the automatically extracted CORONA DEM with height information that has been derived from independent methods such as photogrammetrically-derived contour lines and Shuttle Radar Topography Mission (SRTM) data derived by interferometry.

For the comparison of the SRTM and CORONA DEMs, the ERDAS Imagine® utility "change detection" was used (or "image differencing"). The SRTM DEM was assigned the *after image* character, and the CORONA DEM the *before image* in the formula: Before image – After image = Final image. The final image gets the smaller pixel size (in our case, the CORONA DEM: 17 m) through a nearest neighbor approach

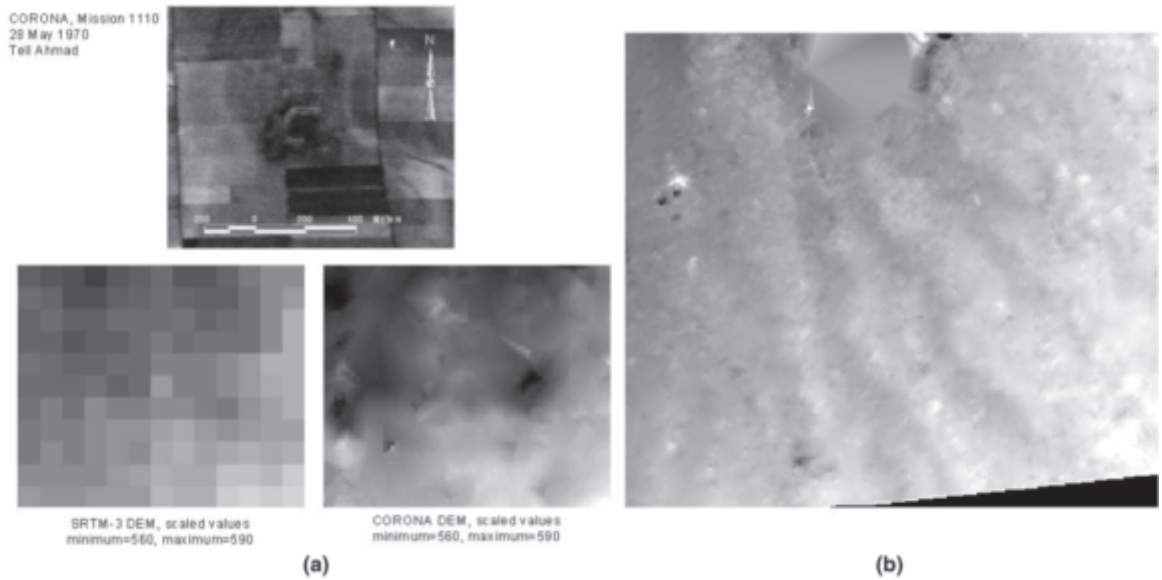

Figure 5. (a) identification of archaeological features, and (b) detection of river channels.

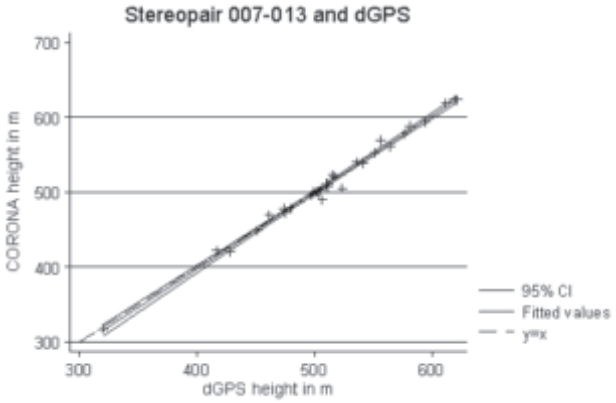

Figure 6. plot of the relationship between the DGPS heights and height data from the CORONA DEM.

and its boundaries are defined by the use of AOI (Area Of Interest) layer. Table 4 and Figure 7 display the results.

The results show large differences at the edges (maximum/minimum) of the points' distribution. However, this applies to a very small number of points and this can be seen from the statistic of the percentage of pixels within one standard deviation of the mean DEM altitude. The mode of the distribution shows less than a one meter difference, and the mean altitudinal differences for the three DEMs are 3.30, 2.24, and 1.30 meters, respectively. This shows a very good fit between the SRTM three arcsec and the CORONA DEMs. It should be noted that in the SRTM three arcsec DEM of the Homs area, a few locations were blank where the river has steep banks and the height values were anomalous.

Direct comparison with SRTM three arcsec data is problematic because of the difference in spatial resolution between the DEMs. However, after resampling the CORONA DEM to the SRTM three arcsec resolution, statistical analysis using all pixels from three stereopairs except the masked out lake, cloud, and cloud shadow areas. This reduced the number of points for the correlation and regression statistics to run. The DEMs are strongly correlated $R^2 = 0.984$ overall, stereopair 009-015 has the best fit $R^2 = 0.975$ (see Table 5). Figure 8a shows the $y = x$ relationship for all the stereopairs using all of the data without any attempt to filter out unwanted artifacts. Figure 8b shows an excellent fit with residuals only present at the lowest elevation values. Figures 8c and 8d reveal a number of distinctive vertically structured points that appear to be associated with errors in the CORONA DEM.

Figure 9 shows the spatial distribution of residuals from the linear fit of the 007-013 stereopair (Figure 8d) in order to investigate the cause of the vertically structured residual

TABLE 4. STATISTICAL SUMMARY OF THE CORONA AND SRTM THREE ARCSEC DEM COMPARISON

Statistics	*007013-SRTM*	*008014-SRTM*	*009015-SRTM*
Maximum (m)	128.57	89.43	92.39
Minimum (m)	−125.97	−93.27	−50.74
Mean (m)	3.30	2.24	1.30
Median (m)	1.98	1.32	−0.59
Mode (most frequently occurring)	−0.70	0.34	−0.47
Standard Deviation	8.98	7.97	5.03
Pixels in one standard deviation	81.36%	71.94%	77.37%
Total number of overlap pixels	1,125,898	1,064,586	126,9917

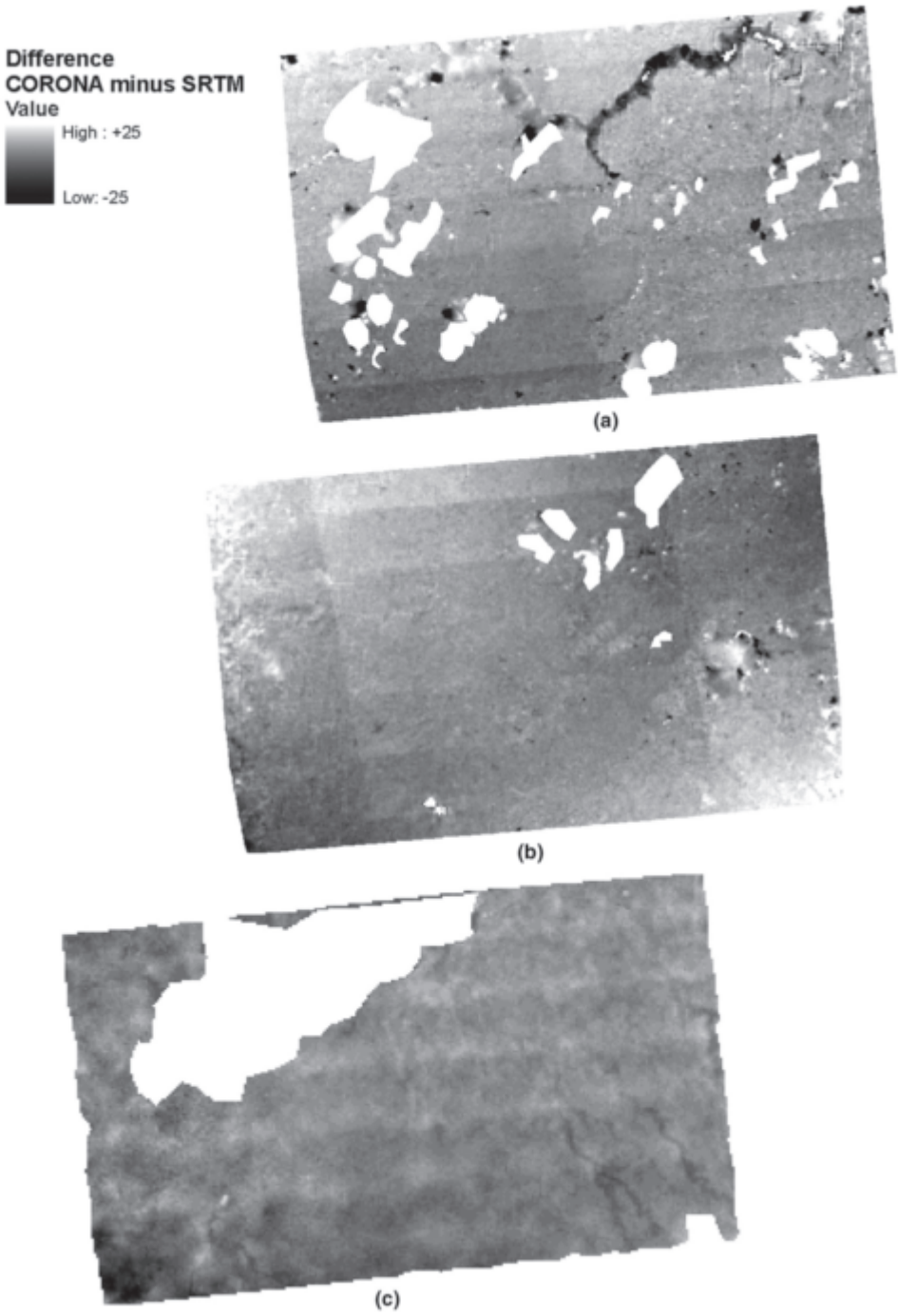

Figure 7. Difference images CORONA minus SRTM: (a) from 007-013 stereopair, (b) from 008-014 stereopair, and (c) from 009-015 stereopair.

TABLE 5. STATISTICAL SUMMARY OF FIGURE 8

Statistics	007013-SRTM	008014-SRTM	009015-SRTM	All Stereopairs
Total number of overlap pixels	33,270	37,986	29,595	100,851
Correlation (r)	0.964	0.966	0.987	0.992
Regression (R^2)	0.930	0.934	0.975	0.984

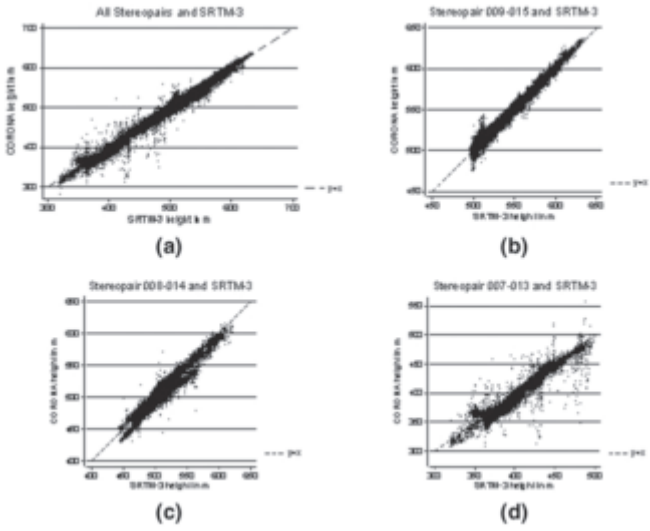

Figure 8. Scatterplot of CORONA stereopairs and SRTM three arcsec data showing $y = x$ relationship: (a) all stereopairs and SRTM-3, (b) stereopair 009-015 and SRTM-3, (c) stereopair 008-014 and SRTM-3, and (d) stereopair 007-013 and SRTM-3.

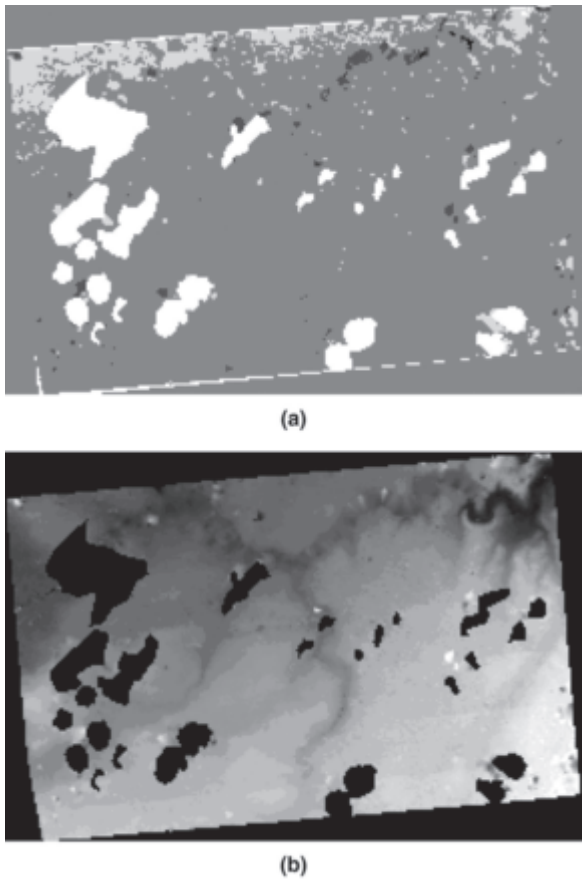

Figure 9. (a) Map of residuals from 95 percent confidence interval from linear fit between CORONA 007-013 and SRTM three arcsec data, and (b) DEM from 007-013 stereopair.

values. The dark and light grey regions on the map of Figure 9 represent areas with residual values greater than the 95 percent confidence interval. The white regions represent clouds and cloud shadows. The black regions are SRTM three arcsec voids which correspond to some lakes and the steep wadi side slopes of an Orontes tributary. The grey values fall within the 95 percent confidence interval. The pattern of residuals shows the CORONA-SRTM fit is poorest in (a) areas farthest away from ground control points, and (b) in a large wadi channel with steep sides again where ground control is unavailable. The striping or banding effect does not stand out as a major problem from the residual map. These effects are reflected in the slightly reduced R^2 value ($R^2 = 0.93$) but the main source of error seems to be caused by the lack of ground control. Otherwise, the statistical comparison of the two DEMs shows good agreement.

The relationship between the DEMs is also shown in the quantile-quantile plot of the two height fields (Figure 10) which shows that, relative to SRTM three arcsec, CORONA under represents height over the altitudinal range 350 m to 400 m. The quantile-quantile plot is a commonly used statistical tool for identifying bias between two variables. In effect, it normalizes the height distribution data so that it can be visualized as an $x = y$ linear fit between variables. It is important to remember that both DEMs are derived from remote sensing and so incorporate error. Given all the possible sources of error, relationship between CORONA and SRTM three arcsec appears very linear and unbiased. What is reassuring is that the CORONA DEM shows good quantitative agreement with two independent height data sets.

Having established the validity of the height data, it is helpful to examine the information contained within the DEM in more detail. We derived slope and contour maps from the 17 m CORONA DEM to see whether there was any significant difference with the SRTM three arcsec data set. A qualitative illustration of the slope information is shown in Figure 11 where the right hand side of the figure shows the overlay of 20 m vertically spaced contour lines derived from both DEMs. The thick dark areas are actually voids of the SRTM data because of the steep wadi side slopes of the Orontes river tributary. The thick straight line shows the location of the height profiles across the line for map contour lines (top), the SRTM (middle), and the CORONA (bottom). The profiles illustrate the difference in pixel size

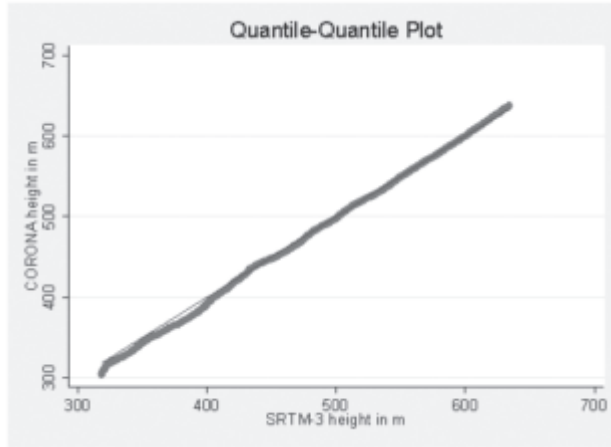

Figure 10. Quantile-quantile plot of CORONA 007-013 stereopair and SRTM three arcsec height data showing linear fit.

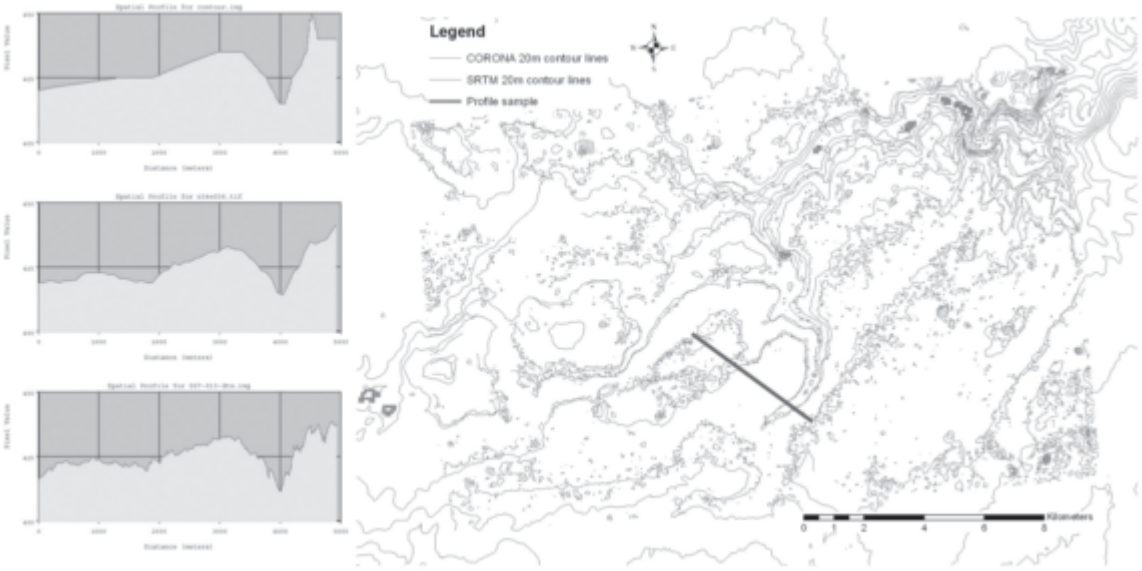

Figure 11. A comparison of contours and vertical profiles from the CORONA 007-013 and *SRTM* three arcsec data. A color version of this figure is available at the ASPRS website: **www.asprs.org**.

between the DEMs where CORONA appears to show a greater level of detail compared to the others. This detail may be important for identifying topographic features particularly local drainage patterns. It is important to remember that as well as scale differences among these data, the CORONA data is 35 years older than the SRTM data and it is possible that some features have been smoothed by geomorphological processes. In plan view it is reassuring to see that the contour patterns match relatively well although the CORONA data contains detail that may be regarded as noise.

Figure 12 shows a comparison of rasterized slope maps from the two DEMs. The dotted box on the Figure 12a image shows the spatial extent of the area of interest defined by the CORONA stereopair coverage, outside this box on the Figure 12b image is SRTM data. The lines within the area of interest show extreme slope values which in this case depict cloud and cloud shadow areas that were masked prior to DEM extraction. The spots in SRTM slope map are voids or missing data presumably due to radar shadow in the larger wadis. This comparison again shows good qualitative agreement and some of the circular features in the CORONA data correspond with known large tell sites, only one of which is seen on the SRTM data.

These comparisons provide confidence that the CORONA DEM is of good quality and useful for environmental applications. The data we present includes all the errors that are inherent in the CORONA pre-processing (misregistration, different ground resolution, and possible scanning errors) and automatic DEM extraction. It is likely that errors could be further reduced with the use of well distributed DGPS ground control measurements.

Also, when comparing (see Table 6), our results with the results of the Moroccan studies which used DGPS ground control (Altmaier and Kany, 2002), it is interesting to note that in spite of the difficulties in obtaining control points, both the positional and altitudinal residuals are better.

Other researchers have attempted to improve the accuracy of DEM extraction accuracy by first stratifying the imagery by land-cover type (Buyuksalih *et al.* (2005). This is a useful techniques in urban or forested areas may for

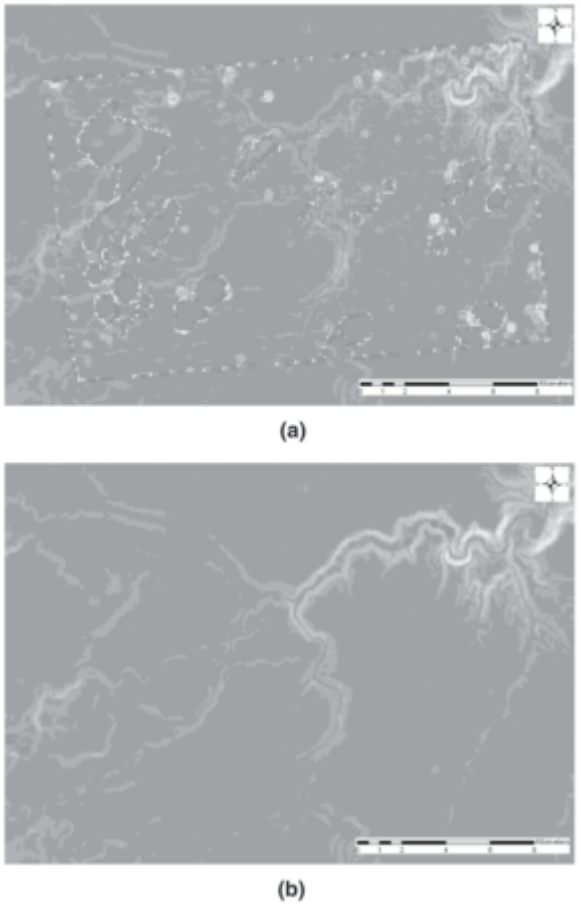

Figure 12. Slope comparison between (a) CORONA, and (b) SRTM DEMs.

TABLE 6. RESIDUALS COMPARISON

Homs project DEM site (this study)			Morocco DEM site		
007-013 // 12 control points			8 control points		
mX	mY	mZ	mX	mY	mZ
2.76 m	2.80 m	2.00 m	9.83 m	9.17 m	3.38 m
008-014//15 control points			8 control points		
mX	mY	mZ	mX	mY	mZ
2.22 m	4.78 m	5.49 m	6.37 m	6.37 m	1.52 m
009-015 // 17 control points					
mX	mY	mZ			
5.35 m	6.59 m	1.02 m			

example, but our study has seen no land-cover change that have resulted in height differences.

Conclusions

CORONA can be used to derive accurate height information; the process is repeatable and can be achieved even with relatively little ground control. If good quality map data are not available, the Ikonos Geo product satellite imagery offers a good base-layer for horizontal control. By registering the maps to Ikonos, height information becomes available. Notice that no field measurements were used for the DEM production from CORONA data.

Satellite ephemeris, attitude data, and specialist panoramic image processing software, all of which are difficult to obtain, are not in fact necessary to generate DEMs from CORONA stereo imagery.

It is important to be aware of CORONA image characteristics which might impact on photogrammetry. No two CORONA missions were identical. In many missions with stereoscopic capability, the two camera systems (aft and forward) were different. If scanned with care, the CORONA image quality can provide high levels of detail on ground features. The scanning should be done using a photogrammetric scanner for best geometric and radiometric results. The geometric resolution of the scanning should be done in balance with the radiometric precision if the user wishes to get the most from the imagery. Also, the scanner should be sufficiently calibrated and the scanning parameters should be kept the same between image pairs. CORONA DEMs are most valuable at locations where conventional maps are difficult to obtain, and so validation of the CORONA DEM in such areas is problematic. SRTM DEM provides an independent source of data to validate the CORONA DEM. In this study, the CORONA DEM was compared with the SRTM data to give a quantitative assessment of accuracy. This helps to evaluate the overall reliability of the photogrammetry applied to imagery from the CORONA cameras.

The CORONA DEM data compares well with other sources of height data and the methodology appears to be robust. The quality and indeed capability of CORONA to generate accurate DEMs still needs to be tested in more situations.

Acknowledgments

Nikolaos Galiatsatos gratefully acknowledges the support of his respective funding body: the Hellenic State Scholarship Foundation, Specialty T1327.06, Contract 368. Many thanks to Bob Taft of Leica Geosystems for providing the panoramic model for SocetSet™, to Dr. John Mills of Newcastle University for use of SocetSet™ in his laboratory, to The Council for British Research in the Levant, and to the Research Committee of the University of Durham for financial and logistical support. Particular thanks are due to Professor Sultan Muhesen and Dr. Abd el-Razzaq Muath, Directors General of Antiquities and Museums (DGAM) in Damascus and their staff who have helped the project in numerous ways. Local support has been provided by Mr. Farid Jabour and Ms. Maryam Bshesh of the Homs office of the DGAM. The authors appreciate the helpful and detailed comments given by anonymous reviewers.

References

Altmaier, A., and C. Kany, 2002. Digital surface model generation from CORONA satellite images, *ISPRS Journal of Photogrammetry and Remote Sensing*, 56(4):221–235.

Beck, A.R., G. Philip., D.N.M. Donoghue., and N. Galiatsatos, 2005. Geo-locating CORONA imagery for archaeological surveys and cultural resource management: A case study in Syria, *Volo nel Passato: Aerofotografia e Cartografia Archeologica* (C. Musson, R. Palmer and S. Campana, editors), All'Insegna del Giglio.

Buyuksalih, G., G. Kocak, and M. Oruc, 2005, Geometric accuracy evaluation of the DEM generated by the Russian TK-350 stereo scenes using the SRTM X- and C-band interferometric DEMs, *Photogrammetric Engineering & Remote Sensing*, 71(11): 1295–1301.

Bindschadler, R., and P. Vornberger, 1998. Changes in the west Antarctic ice sheet since 1963 from declassified satellite photography, Science, Vol. 279, pp. 689–692.

Bridgland, D.R., G. Philip, R. Westaway, and M. White, 2003. A long Quaternary terrace sequence in the Orontes river valley, Syria: A record of uplift and of human occupation, *Current Science*, 84(8):1080–1089.

Case, J.B., 1967. The analytical reduction of panoramic and strip photography, *Photogrammetria*, pp. 127–141.

Davis, C.H., and X. Wang, 2003. Planimetric accuracy of Ikonos 1 m panchromatic orthoimage products and their utility for local government GIS basemap applications, *International Journal of Remote Sensing*, 24(22):4267–4288.

Day, D.A., J.M. Longson, and B. Latell (editors), 1998. *Eye in the Sky – The Story of CORONA Spy Satellites*, Smithsonian Institution Press, Washington, D.C. and London.

Deveraux, Jr., A.B., 1973. *Investigations into the Feasibility of Employing a Hypothetical Panoramic Frame Camera System in Aerial Triangulation*, Ph.D. dissertation, Ohio State University, Geodesy Department.

Farr, T., 2004. Reply in the discussion forum for users of SRTM data, URL: http://pub7.bravenet.com/forum/537683448/fetch/394357/(last date accessed: 08 May 2008).

Förstner, W., and E. Gülch, 1987. A fast operator for detection and precise location of distinct points, corners and centers of circular features, *Intercommission Conference on Fast Processing of Photogrammetric Data*, Interlaken, Switzerland, pp. 281–305.

Fowler, M.J.F., 2004. Declassified CORONA KH-4B satellite photography of remains from Rome's desert frontier, *International Journal of Remote Sensing*, 25(18):3549–3554.

Fraser, C.S., H.B. Hanley, and T. Yamakawa, 2002. Three-dimensional geopositioning accuracy of IKONOS imagery, *The Photogrammetric Record*, 17(99):465–479.

Galiatsatos, N., 2004. *Assessment of the CORONA Series of Satellite Imagery for Landscape Archaeology: A Case Study from Orontes Valley*, Syria, Ph.D. dissertation, Durham University, Geography Department, United Kingdom.

Gerlach, F., 2000. Characteristics of Space Imaging's one-meter resolution satellite imagery products, *International Archives of Photogrammetry and Remote Sensing*, Amsterdam, Vol. 33, Part B1.

Gonçalves, J., and J.C. Fernandes, 2005. Assessment of SRTM-3 DEM in Portugal with topographic map data, *Proceedings of the EARSeL Workshop 3D-Remote Sensing*, 10–11 June, Porto, Portugal (European Association of Remote Sensing Laboratories), unpaginated CD-ROM.

Goossens, R., M. Schmidt, A. Altmaier, F. Benoit, and G. Menz, 2001. Extraction of digital elevation models and ortho-images from CORONA KH4B data, *Proceedings of ISPRS Workshop: High Resolution Mapping from Space*, Hanover, Germany.

Grodecki, J., G. Dial, and J. Lutes, 2003. Block adjustment of high resolution satellite images described by rational polynomials, *Photogrammetric Engineering & Remote Sensing*, 69(1):59–68

Jacobsen, K., 2005. Analyses of SRTM elevation models, *Proceedings of the EARSeL Workshop 3D-Remote Sensing*, 10–11 June, Porto, Portugal (European Association of Remote Sensing Laboratories), unpaginated CD-ROM.

Kasser, M., 2002. Use of scanners for the digitisation of aerial pictures, *Digital Photogrammetry* (M. Kasser and Y. Egels, editors), Taylor and Francis, London and New York.

Kay, S., P. Spruyt., R. Zielinski, P. Winkler, S. Mihály, and G. Ivan, 2005. Quality checking of DEM derived from satellite data (SPOT and SRTM), *Proceedings of the EARSeL Workshop 3D-Remote Sensing*, 10–11 June, Porto, Portugal (European Association of Remote Sensing Laboratories), unpaginated CD-ROM.

Madden, F.J., 1996. The CORONA camera system: ITEK's contribution to world stability, self-published monograph.

Leachtenauer, J.C., K. Daniel, and P.T. Vogl, 1997. Digitizing Corona imagery: Quality vs. cost, *CORONA Between the Sun and the Earth – The First NRO Reconnaissance Eye in Space* (R.A. McDonald, editor), American Society for Photogrammetry and Remote Sensing, Bethesda, Maryland.

McDonald, R.A., 1995. CORONA: Success for space reconnaissance, a look into the Cold War, and a revolution for intelligence, *Photogrammetric Engineering & Remote Sensing*, 61(6):689–720.

McDonald, R.A. (editor), 1997. *CORONA Between the Sun and the Earth - The First NRO Reconnaissance Eye in Space*, American Society for Photogrammetry and Remote Sensing, Bethesda, Maryland.

Menze, B.H., J.A. Ur, and A.G. Sherratt, 2006. Detection of ancient settlement mounds - Archaeological survey based on the SRTM based model, *Photogrammetric Engineering & Remote Sensing*, 72(3):321–327.

National Reconnaissance Office (NRO), 1967. *The KH-4B Camera System*, National Photographic Interpretation Center, September.

National Reconnaissance Office (NRO), 1970a. *CORONA Technical Information*, Volume 1, National Photographic Interpretation Center, December.

National Reconnaissance Office (NRO), 1970b. CORONA technical information, Volume 2, National Photographic Interpretation Center, December 1970.

Palmer, R., 2002. A poor man's use of CORONA images for archaeological survey in Armenia, *Proceedings of the Conference: Space Applications for Heritage Conservation*, Strasbourg, France.

Peebles, C., 1997. *The CORONA Project: America's First Spy Satellites*, Naval Institute Press, Annapolis, Maryland.

Philip, G., D.N.M. Donoghue, A. Beck, and N. Galiatsatos, 2002a. CORONA satellite photography: A case study from Orontes Valley, Syria, *Antiquity*, 76:109–118.

Philip, G., F. Jabour, A. Beck, M. Bshesh, J. Grove, A. Kirk, and A. Millard, 2002b. Settlement and landscape development in the Homs region, Syria: Research questions, preliminary results 1999–2000 and future potential, *Levant*, 34:1–23.

Philip, G., M. Abdulkarim, P. Newson, A. Beck, D. Bridgland, M. Bshesh, A. Shaw, R. Westaway, and K. Wilkinson, 2005. Settlement and landscape development in the Homs Region, Syria: Report on work undertaken during 2001–2003, *Levant*, Vol. 37.

Polidori, L., 2002. DSM quality: Internal and external validation, *Digital Photogrammetry* (M. Kasser and Y. Egels, editors), Taylor and Francis, London and New York.

Rabus, B., M. Eineder, A. Roth, and R. Bamler, 2003. The shuttle radar topography mission – A new class of digital elevation models acquired by spaceborne radar, *ISPRS Journal of Photogrammetry and Remote Sensing*, 57:241–262.

Ratcliffe, I.C., and G.M. Henebry, 2004. Using declassified intelligence satellite photographs with QuickBird imagery to study urban land cover dynamics: A case study from Kazakhstan, *Proceedings of the ASPRS Annual Conference*, Denver Colorado, unpaginated CD-ROM.

Ruffner, K. (editor), 1995. *CORONA: America's First Satellite Program*, Center for the Study of Intelligence, Government Printing Office, Washington, D.C.

Schenk, T, B. Csathó, and S.W. Shin, 2003. Rigorous panoramic camera model for DISP imagery, *Proceedings of the ISPRS Workshop: High Resolution Mapping from Space*, Hanover, Germany.

Schmidt, M., R. Goossens, and G. Menz, 2001a. Processing techniques for CORONA satellite images in order to generate high-resolution digital elevation models (DEM), *Observing Our Environment from Space: New Solutions for a New Millennium* (G. Begni, editor), Lisse, The Netherlands, pp. 191–196.

Schmidt, M., R. Goossens, G. Menz, A. Altmaier, and D. Devriendt, 2001b. The use of CORONA satellite images for generating a high-resolution digital elevation model, *Proceedings of the 2001 IGRASS Symposium*, Sydney.

Schneider, T., K. Jacobsen, R. Seitz, and B. Förster, 2001. Remote sensing based parameter extraction for erosion control purposes in the Loess plateau of China, *Proceedings of the ISPRS Workshop: High Resolution Mapping from Space 2001*, Hanover, Germany.

Selander, J.M., 1997. Image coverage models for declassified CORONA, ARGON and LANYARD satellite photography – A technical explanation, *CORONA Between the Sun and the Earth The First NRO Reconnaissance Eye in Space* (R.A. McDonald, editor), American Society for Photogrammetry and Remote Sensing, Bethesda, Maryland.

Shin, S.W., 2003. *Rigorous Model of Panoramic Cameras*, Ph.D. dissertation, Department of Civil and Environmental Engineering and Geodetic Science, Ohio State University, 104 p.

Slama, C.C., C. Theurer, and S.W. Henriksen (editors), 1980. *Manual of Photogrammetry*, American Society of Photogrammetry.

Sohn, H.G., G. Kim, J. Yom, 2004. Mathematical modelling of historical reconnaissance CORONA KH-4B imagery, *The Photogrammetric Record*, 19(105):51–66.

Space Imaging, 2005. Ikonos product guide. URL: http://www.geoeye.com/products/imagery/ikonos/default.htm (last date accessed: 08 May 2008)

Tappan, G.G., A. Hadj, E.C. Wood, and R.W. Lietzow, 2000. Use of Argon, Corona and Landsat imagery to assess 30 years of land resource changes in west-central Senegal, *Photogrammetric Engineering & Remote Sensing*, 66(6):727–735.

Thom, C., 2002. Relations between radiometric and geometric precision in digital imagery, *Digital Photogrammetry*, (M. Kasser and Y. Egels, editors) Taylor and Francis, London and New York.

Ur, J., 2003. CORONA satellite photography and ancient road networks: A northern Mesopotamian case study, *Antiquity*, 77(295):102–115.

(Received 04 August 2006; accepted 16 October 2006; revised 12 January 2007)